E-proceedings of the 38th IAHR World Congress
September 1-6, 2019, Panama City, Panama
doi:10.3850/38WC092019-1004

STUDY ON RELATIONSHIP BETWEEN LATERAL OVER FLOW AND ITS LOCATION OF LATERAL WEIR IN CURVED CHANNEL

KOJI ASAI[(1)], NOBUYUKI KAWAMOTO[(2)] , TATSUYA SHIROMIZU [(3)] & HAJIME SHIROZU[(4)]

[(1,2,4)] Yamaguchi University, Ube, Japan,
e-mail: kido@yamaguchi-u.ac.jp[(1)], morzalt@yamaguchi-u.ac.jp[(2)], shiro@yamagiuchi-u.ac.jp[(4)]

[(3)] Kyushukensetsu Consultant co.,ltd, Fukuoka, Japan,
e-mail: tatsuya.shiromizu@qcon.co.jp

ABSTRACT

The characteristic of the lateral over flow was investigated with the curved channel which has the constant radius of curvature R. The curved channels with R=0.50m and 7.0m were used. The main results obtained from these experiments are as follows; (1) The lateral over flow discharge is proportional to the power of the over flow depth. The power is around 3/2 if the lateral wire is set near the entrance of the curved channel. The value of the power decrease as the location of the lateral wire is installed downward. (2) The ratio of the lateral over flow discharge with the inflow discharge does not well depend on the location of the weir from the entrance to the middle part of the channel. In downstream wise from the middle the ratio decreases. (3) The ratio of R=0.50m is larger than that of R=0.70m. (3) We applied the lateral discharge formulation we proposed in 2017 to the experimental data. It is observed that it has a good accuracy except near the entrance and the exit of the curved channel.

Keywords: lateral over flow, curved channel, radius of curvature, location of lateral weir

1 INTRODUCTION

The studies on the distribution of discharge with the lateral over flow weir have been related to the water supply to the irrigation channel from the river, the leading flood to the flood plain dam as a river flood control measure. The lateral over flow in the straight open channel, generally, are targeted at these researches, so that there are so many researches on the lateral over flow in the straight channel, for example, De Marchi. (1934), Ranga. et al (1979), Murota A. et al (1985) Hager (1987), Onitsuka et al (2005, 2007), Vatankhah (2013), Yilmaz (2001). Moreover, it is anticipated that heavy rain disasters increase by the global warming. Now a days, "the reduction of disaster" become more important. The term of the reduction of disaster is not only to prevent of disasters but also to reduce disasters. In other words, it is minimization of disasters. As one of countermeasures of the reduction of disasters hazard maps or risk maps are very useful. One of the important contents of hazard maps is a predicted inundation map. In Japan, the predicted inundation map is created by numerical flood simulations under the assumption that the river dike is broken at an arbitrary position.

The inflow discharge from the broken dike as a boundary condition is evaluated by the lateral over flow formulation for the straight channel. However, the broken position of the dike is not always at a straight part of the river dike but also at the meandering part. There is a room to improve the lateral over flow formulation to apply it to a meandering broken position. Recently, the development of the numerical inundation simulation technique enables us to make a more precious inundation simulation including the river flow. It means that no lateral over flow formulation is required to make a flood inundation simulation. However, it is important, from the academic view point, to study the characteristics of the lateral over flow from the meandering channel.

Based on this background, we have been studied on the lateral flow, the lateral over flow formulation. Generally, the radius of the curvature of the real meandering river varies. We used the curved channel of which the radius of the curvature is constant as the fundamental study. Asai and Kawamoto (2017) studied on the characteristics of the lateral overflow in the curved channel. In this study the broken point at only θ=90 (see Fig.1) was chosen because the flow impact would take maximum at this point. However, this point is not always a broken point. Other positions can be broken points. It could be easily anticipated that the characteristics of the over flow depends on the position of the broken point. Therefore, it is important to study the dependence of the lateral over flow characteristics on the position of the broken point. We studied the relationship between the lateral over flow characteristics and the position of the broken point with the curved channel having the constant radius of the curvature. We would like to note that we have considered dike failure problems in real rives, but here we have regarded dike failure problems as lateral over flow problems from a lateral side weir.

©2019, IAHR. Used with permission / ISSN 2521-7119 (Print) - ISSN 2521-716X (Online) - ISSN 2521-7127 (USB)

2 EXPERIMENTAL SETUP

Figure 1 shows the schematic view of the experimental channel. The curved channel consists of two straight channel parts and the bend channel part. This curved channel is made of the acryl grass. The channel bed slope is set to be 0 (flatbed slope). The width B is 0.20m. The length of the straight channel in the upstream side is 1.40m and that in the downstream side is 1.10m. R is the radius of curvature. The length L of the lateral side weir is also 0.20m. θ is the angular measured from the entrance of the bend part to the center of the lateral weir as shown in figure 1. θ is one of important parameters in this research. The bend channel part is divided into five parts as shown in figure 1. We have prepared five parts installing no lateral side weir and those installing the lateral side weir. The position of the lateral over flow can be changed by setting the part having the lateral side weir. Table 1 shows the parameter R and θ used in our experiments. Unit of θ used here is degree.

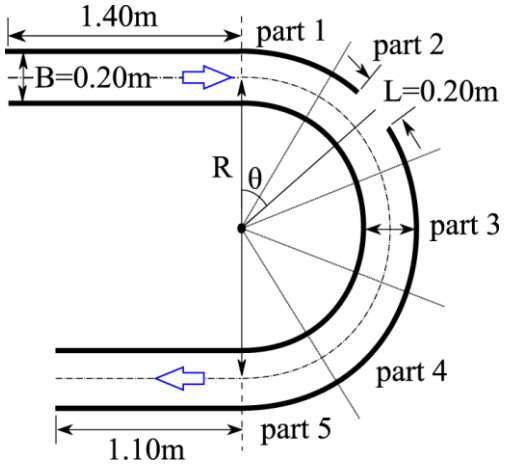

Figure 1 Over view of curved channel

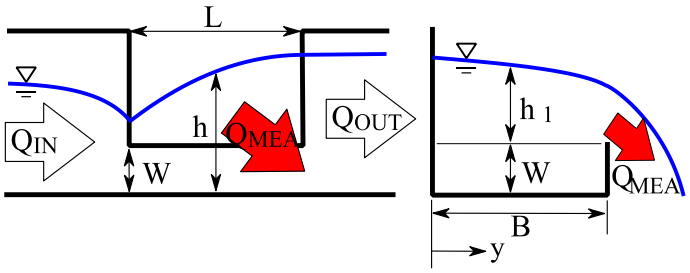

Figure 2 Schematic view of lateral side weir

Table 1 Parameter R and θ

R(m)	θ (°)
0.50, 0.70	18, 54, 90, 126, 162

Table2 Experimental condition

Shape of weir		Inflow discharge
L(m)	W (m)	Q_{IN}(m^3/s)
0.20	Full, 0.055, 0.045, 0.035, 0.025, 0.015, 0.005, 0.000	0.0043, 0.0036 0.0030, 0.0020

Figure 2 shows the schematic view of the lateral side weir. The sharp-crested weir is used. Q_{IN} is the inflow discharge, Q_{OUT} is the out flow discharge and Q_{MEA} is the lateral over flow discharge, W is the weir height, L is the length of the lateral weir, h is the water depth measured at the center of the channel, h_1 is the over flow

©2019, IAHR. Used with permission / ISSN 2521-7119 (Print) - ISSN 2521-716X (Online) - ISSN 2521-7127 (USB)

depth measured at the center of the channel, h is the water depth. The bed slope of the channels is set to be 0, so the water depth h is also the water level H measured from the channel bed.

The experimental conditions are shown in Table 2. Full means the weir height at which no lateral over flow occurs in the column of W in Table 2. L is fixed to be 0.20m which is the same as B. In the case of no lateral over flow the aspect ratio B/h ranged from 3.18 to 5.42.

3 EXPERIMENTAL RESULT

3.1 Hydraulic characteristics of curved channel

Figure 3 shows the transversal water depth profile for R=0.50m, θ=54°, Q_{IN}=0.0043m^3/s. The vertical axis indicates the water depth normalized by the water depth at the nearest inner wall (right side wall against the flow direction) $h_{y=0.02m}$, and the horizontal axis indicates the distance in the transvers direction y normalized by the channel width B. It is well known that the flow in the downstream direction induces the centrifugal force. In the case of no lateral discharge (W=Full) the water depth h increases in y direction due to the centrifugal force. For the non-dimensional weir height 1-W/L=0.825 and 0.875 the transversal water depth profiles are the same as W=Full. On the other hand, the transversal water depths decrease in y direction for 1-W/L=0.975 and1.000.

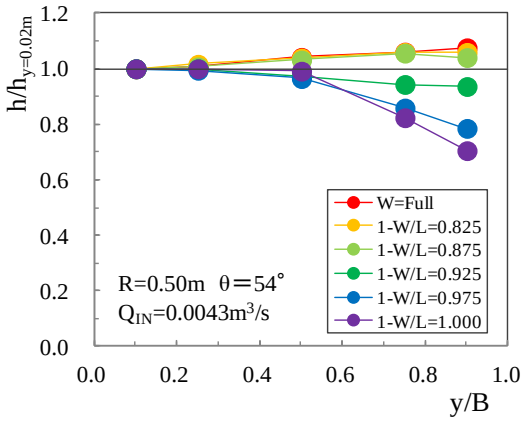

Figure 3 Transversal water depth profile

It is well known that the over flow discharge is in proportion to the power 3/2 of the over flow depth h_1 if the cross section of the weir is rectangular for the front over flow. We tried to check that our experimental results had this property. Figure 4 shows the relationship between the lateral over flow discharge Q_{MEA} and the over flow depth h_1 with the parameter θ. the circular marks mean the experimental results and the solid lines mean the fitting curves. The over flow discharge is almost in proportion to the power 3/2 of h1. However, the proportional power becomes smaller than 3/2 with the increasing θ.

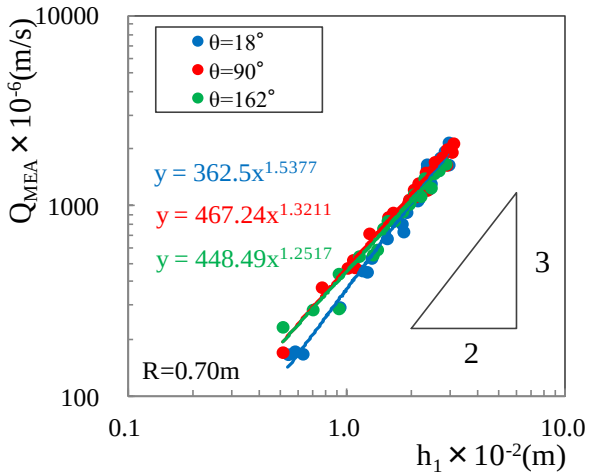

Figure 4 Relationship between the lateral over flow discharge Q_{MEA} and the over flow depth h_1

Figure 5 shows the proportional power T versus θ. In the case of R=0.50m T takes around 1.5 at θ=18° and then T decrease until θ=90°. T takes the constant value 1.2 if θ is over 90°. On the other hand, in the case

©2019, IAHR. Used with permission / ISSN 2521-7119 (Print) - ISSN 2521-716X (Online) - ISSN 2521-7127 (USB)

of R=0.70m the tendency of T with θ is almost the same as R=0.50m, but T increases at θ=120°. T for R=0.50m is a little bit smaller than T for R=0.70m.

3.2 Lateral over flow discharge

Figure 6 shows the relationship between the lateral over flow discharge and θ. The vertical axis indicates the ratio of the lateral over flow discharge to the inflow discharge Q_{MEA}/Q_{IN} (here after the overflow-inflow ratio), and the horizontal axis indicates θ.

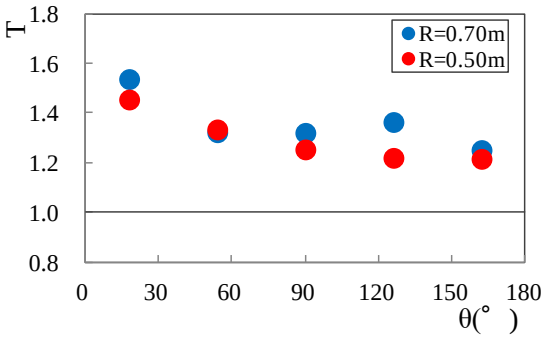

Figure 5 Proportional power T versus q

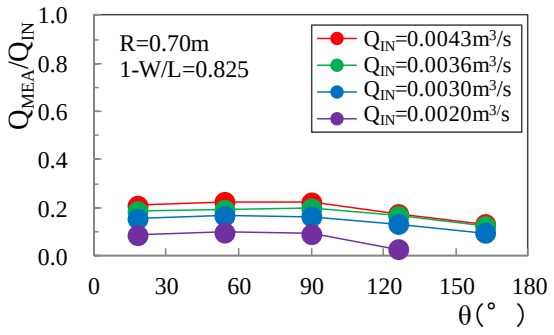

(a) 1-W/L=0.825

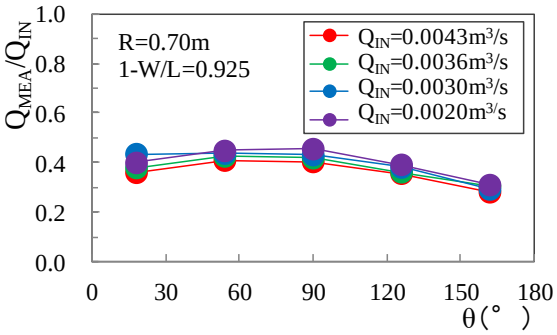

(b) 1-W/L=0.925

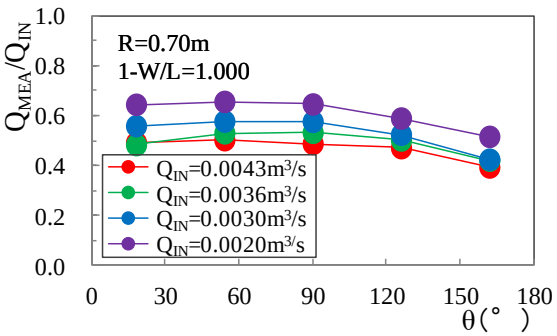

(c) 1-W/L=1.000

Figure 6 Relationship between the lateral over flow discharge and θ

©2019, IAHR. Used with permission / ISSN 2521-7119 (Print) - ISSN 2521-716X (Online) - ISSN 2521-7127 (USB)

Figure 6(a) shows the results for 1-W/L=0.825. There was no lateral over flow at θ=162° for Q_{IN}=0.0020m^3/s because of small inflow discharge. The overflow-inflow ratios for each inflow discharge are constant until θ=90°. The overflow-inflow ratios decrease if θ is greater than 90°, and the greater the overflow-inflow ratio is the greater the inflow discharge is. The maximum value of the overflow-inflow ratio is 0.2.

Figure 6(b) shows the results for 1-W/L=0.925. The maximum value of the overflow-inflow ratio is around 0.4 because of the low weir height. The tendency of the overflow-inflow ratio with θ is the same as the previous weir height, but the discrepancy among inflow discharges is smaller than that for the previous weir height.

Figure 6(c) shows the results for 1-W/L=1.000. The maximum value of the overflow-inflow ratio reaches around 0.6. The tendency of the overflow-inflow ratio with θ is the same as the previous weir heights. However, the tendency for this weir height is in opposition to that for 1-W/L=0.825 in the relationship between the overflow-inflow ratio and the inflow discharge. The overflow-inflow ratio becomes smaller if the inflow discharge increases.

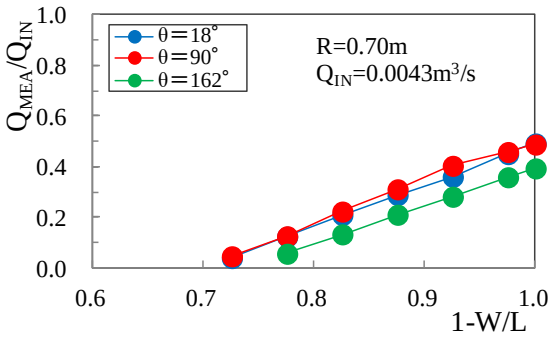

Figure 7 Relationship between overflow-inflow ratio and non-dimensional weir hight

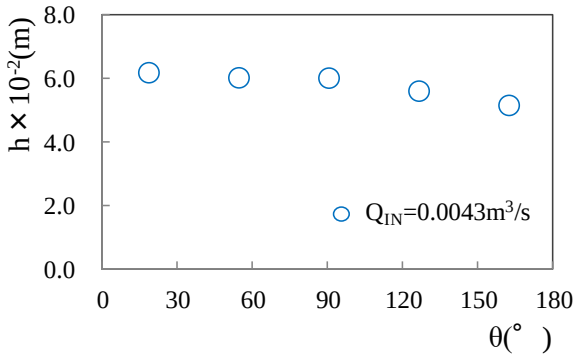

Figure 8 Longitudinal water depth profile with no over flow condition

So far, we discussed the relationship between the lateral over flow discharge and θ with only three weir height. Here, the tendencies related to other weir heights are shown in figure 7. The vertical axis indicates the overflow-inflow ratio, and the horizontal axis indicates the non-dimensional weir height 1-W/L. The positions of the over flow are chosen at θ=18°, 90°, 162°. This figure shows the results for R=0.70m and Q_{IN}=0.0043m^3/s which is the maximum inflow discharge in this study.

The overflow-inflow ratio increases lineally with the non-dimensional weir height. The overflow-inflow ratios for θ=18° and 90° take the almost same values with respect to the non-dimensional weir height. The overflow-inflow ratios for θ=162 is smaller than that for θ=18° or 90°. To explain this reason the longitudinal water depth profile for R=0.70m with no over flow condition is shown in figure 8. This experimental channel was set horizontally, so that the water depth decreases in the flow direction. The water depth is almost constant until θ=90°, but the water depth decreases if θ is greater than 90°. It could be anticipated that there is the same tendency for the over flow condition and the over flow depth become small if θ is greater than 90°.

3.3 Lateral over flow discharge

The comparison of the radius of the curvature R for the relationship between the overflow-inflow ratios and θ is shown in figure 9. This figure shows the results for the non-dimensional weir height 1-W/L=1.00 and Q_{IN}=0.0043m3/s. It is found that the overflow-inflow ratios for both the radius of the curvature are bigger than 0.4, and the overflow-inflow ratios for R=0.50m is greater than that for R=0.70 whatever θ is. It might be related to that the centrifugal force for R=0.50m is larger than that for R=0.70m.

©2019, IAHR. Used with permission / ISSN 2521-7119 (Print) - ISSN 2521-716X (Online) - ISSN 2521-7127 (USB)

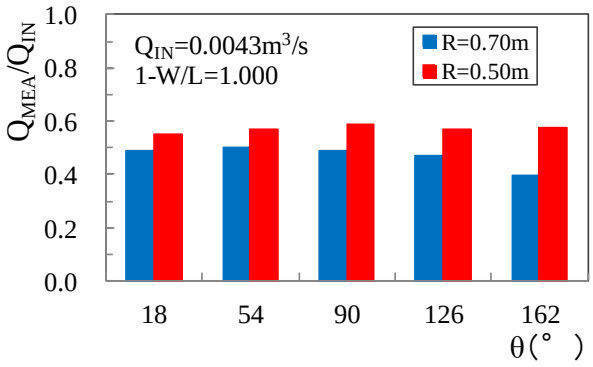

Figure 9 Relationship between the overflow-inflow ratios and θ

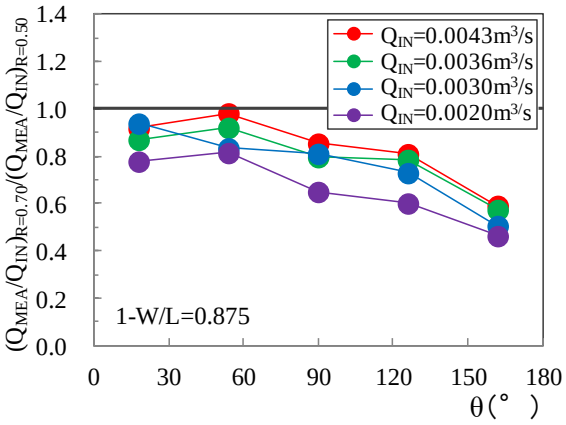

(a) 1-W/L=0.875

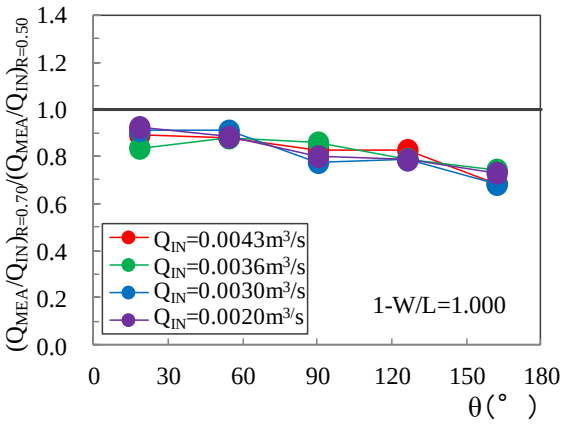

(b) 1-W/L=1.000

Figure 10 Comparison of overflow- inflow ratio with Radius of curvature

The overflow-inflow ratios for R=0.50m are almost constant, while that for R=0.7m decreases if θ is greater than 90°. On the other hand, the water depth for R=0.50m is almost constant. However, it is not clear that it is due to the centrifugal force.

Figures 10 shows the discrepancy between the lateral over flow discharges for R=0.50m and R=0.70m. The vertical axis indicates the ratio of the overflow-inflow ratios for R=0.70m to that for R=0.50m $(Q_{MEA}/Q_{IN})_{R=0.70m}/(Q_{MEA}/Q_{IN})_{R=0.50m}$. The lateral over flow discharge for R=0.70m is smaller than that for R=0.50m if the value of this parameter is less than unity. The horizontal axis indicates θ.

Figure 10(a) shows the results for 1-W/L=0.875. It is found that all the lateral over flow dischargers for R=0.75m are smaller than that for R=0.50m, and this ratio decreases as θ increases. Moreover, there are discrepancies due to the inflow discharge. Figure 10(b) shows the results for 1-W/L=1.000. Similarly, as the previous case, all the lateral over flow dischargers for R=0.70m are smaller than that for R=0.50m. However, the dependence of the inflow discharge is small compering to the previous case.

©2019, IAHR. Used with permission / ISSN 2521-7119 (Print) - ISSN 2521-716X (Online) - ISSN 2521-7127 (USB)

3.4 Lateral over flow discharge formulation

It is not easy to build a reliable lateral over flow discharge formulation for a curved channel because there is not enough data, especially data related to radiuses of curvature. However, we have proposed a simple lateral over flow discharge formulation for a curved channel (Asai, Kawamoto, 2017). Here, we have tried to incorporate the parameter θ into this lateral over flow discharge formulation. The lateral over flow discharge formulation proposed by Asai and Kawamoto is shown in Eq. (1).

$$Q_{CAL} = 0.35 \cdot C_a \cdot \sqrt{2g} \cdot L \cdot h_1^{3/2} \quad [1]$$

where,

$$C_a = C_0 \cdot \left(\frac{L}{B}\right)^0 \cdot \left(1 - \frac{W}{L}\right)^{-0.828} \cdot Fr^{-0.177} \cdot \left(1 - \frac{B}{R}\right)^{-0.239} \quad [2]$$

C_0 is a model coefficient obtained by the experimental data and Asai and Kawamoto (2017) proposed 0.944. the power on L/B is 0. L=0.2m and B=0.2m were used in this paper, so that the number of the non-dimensional parameter L/B is one. They couldn't consider the dependence of this parameter. Fr is the Froude number defined by the sectional averaged velocity and the water depth on the center of the channel. Both hydraulic properties are measured in front of the lateral side weir. Although the lateral over flow discharge is not in proportion to the power 3/2 exactly as shown figure 4, we used Eq. (1) because we have considered that the power is not far from 3/2. And the model coefficient C_0 can be treated as a non-dimensional coefficient by assuming the power 3/2. We include the effect of the position of the lateral side weir θ to the model coefficient C_0. We have obtained the model coefficient C_0 as shown Eq. (3)

$$C_0 = 0.80 \cdot \theta^{0.0677} \quad [3]$$

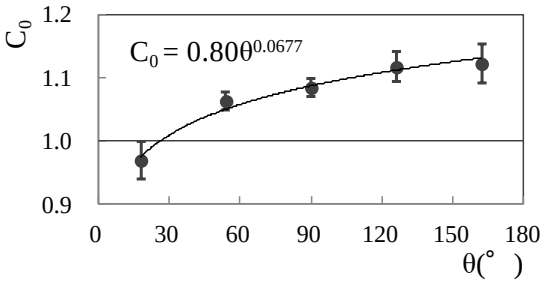

Figure 11 relationship between C_0 and θ

Figure 11 shows the relationship between C_0 and θ. The optimum values of C_0 and the standard deviation of the error are also shown in this figure. The curved line in this figure is Eq. (3). It is found that the Eq. (3) is the best fitting curve. Figure 12 shows the relationship between the measured lateral over flow discharge Q_{MEA} and Q_{CAL} which is the lateral over flow discharge calculated with Eqs. (1), (2) and (3). It is found that the agreement between both discharges are well.

©2019, IAHR. Used with permission / ISSN 2521-7119 (Print) - ISSN 2521-716X (Online) - ISSN 2521-7127 (USB)

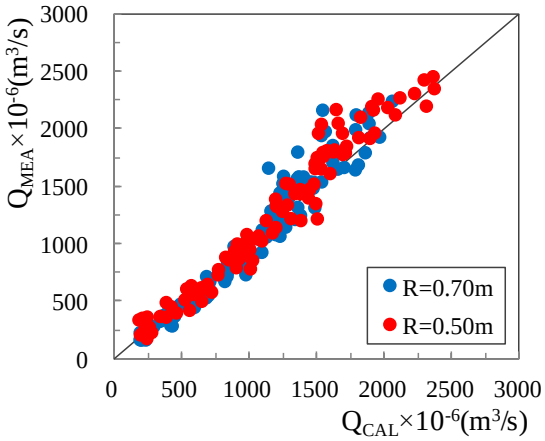

Figure 12 Relationship between calculated discharge and measured discharge

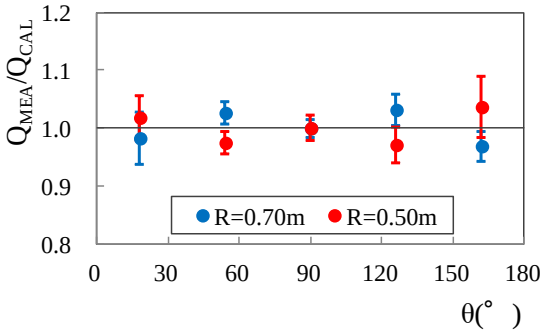

Figure 13 Accuracy of presented lateral overflow discharge formulation with respect to θ

Figure 13 shows the accuracy of presented lateral overflow discharge formulation with respect to θ. The vertical axis indicates the ration of the measured discharge to the calculated discharge, and the horizontal axis indicates the position of the lateral side weir θ. The circle symbols indicate the mean value and the bars indicate the standard deviations of the error. The original coefficient Eq. (2) was optimized for θ=90°, so the results at θ=90° are well. Although the error ranges at θ=54° and 126° are a little bit wider, the mean values are nearly 1.0. The mean values at θ=18° and 62° are nearly 1.0, but the error ranges are wider.

4 CONCLUSIONS

The main conclusions in this study are summarized as follows;

1. The lateral over flow discharge is proportional to the power of the over flow depth. The power is around 3/2 if the lateral wire is set near the entrance of the curved channel. The value of the power decrease as the location of the lateral wire is installed downward. The power for R=0.70m is greater than that for R=0.50m.
2. The ratio of the lateral over flow discharge to the inflow discharge (the overflow-inflow ratio) for R=0.70m decrease if the position of the lateral side weir θ exceeds 90°. On the other hands, the overflow-inflow ratio for R=0.50m does not depend on θ.
3. The overflow-inflow ratio for R=0.50m is greater than that for R=0.70m.
4. The lateral discharge formulation we proposed in 2017 was modified to incorporate the effect of the position of the lateral side weir. It has a good accuracy except near the entrance and the exit of the curved channel.

REFERENCES

Asai K, Kawamoto N (2017). Study on Effect of Radius of Curvature on Lateral over Flow in Curved Channel, E-proceedings of the 37th IAHR World Congress, pp.1361-1368.
De Marchi, G. (1934). Essay on the performance of lateral weirs. L' Energia Elettrica, Milan, Italy, 11, 849-860.
Hager, W.H. (1987). Lateral outflow over side weirs. J. Hydraulic Engineering, 9, 491-504.
Murota A., Fukuhara T., Sukita Y. (1985). Study on Evaluation of Discharge over Side Weirs. Proc. of JSCE, 363/II-4, 249-252 (in Japanese).

©2019, IAHR. Used with permission / ISSN 2521-7119 (Print) - ISSN 2521-716X (Online) - ISSN 2521-7127 (USB)

Onitsuka K., Akiyama J., Tsunematsu T., Mataga M. (2005). Discharge Coefficients of Side-Weirs in Subcritical Open-Channel Flows. J. Hydrau., Coast. Environ. Eng., JSCE, 803/II-73, 81-89 (in Japanese)

Onitsuka K., Akiyama J., Mataga M., Ida C. (2007). Discharge Coefficients of Side-Weirs in Supercritical Open-Channel Flows. Doboku Gakkai Ronbunshu B, 63(2), 134-143 (in Japanese)

Ranga Raju, K.G., Prasad, B. and Gupta, S.K. (1979). Side weir in rectangular channel. J. Hydraulics Division, ASCE, 105, 547-554.

Vatankhah A.R. (2013). Water Surface Profiles along a Rectangular Side Weir in a U-Shaped Channel (Analytical Findings), J. Hydorogic Engineering, 593-602.

Yilmaz Muslu (2001). Numerical Analysis for Lateral Weir Flow, J. Irrig. Drain Eng. 127, 246-253.

©2019, IAHR. Used with permission / ISSN 2521-7119 (Print) - ISSN 2521-716X (Online) - ISSN 2521-7127 (USB)